Emissive Synthetic Cofactors: An Isomorphic, Isofunctional, and Responsive NAD(+) Analogue

Emissive synthetic cofactors: An isomorphic, isofunctional and responsive NAD+ analogue

Alexander R. Rovira, Andrea Fin, Yitzhak Tor

ABSTRACT: The synthesis, photophysics, and biochemical utility of a fluorescent NAD^+ analogue based on an isothiazolo[4,3-*d*]pyrimidine core ($\mathbf{N^{tz}AD^+}$) are described. Enzymatic reactions, photophysically monitored in real time, show $\mathbf{N^{tz}AD^+}$ and $\mathbf{N^{tz}ADH}$ to be substrates for yeast alcohol dehydrogenase and lactate dehydrogenase, respectively, with reaction rates comparable to that of the native cofactors. A drop in fluorescence is seen as $\mathbf{N^{tz}AD^+}$ is converted to $\mathbf{N^{tz}ADH}$, reflecting a complementary photophysical behavior to that of the native NAD^+/NADH. $\mathbf{N^{tz}AD^+}$ and $\mathbf{N^{tz}ADH}$ serve as substrates for NADase, which selectively cleaves the nicotinamide's glycosidic bond yielding $\mathbf{^{tz}ADP\text{-}ribose}$. $\mathbf{N^{tz}AD^+}$ also serves as a substrate for ribosyl transferases, including human adenosine ribosyl transferase 5 (ART5) and Cholera Toxin Subunit A (CTA), which hydrolyze the nicotinamide and transfer $\mathbf{^{tz}ADP\text{-}ribose}$ to an arginine analogue, respectively. These reactions can be monitored by fluorescence spectroscopy, in stark contrast to the corresponding processes with the non-emissive NAD^+.

Modified oligonucleotides represent a fraction of the innovative ways for exploiting fluorescent nucleoside analogues.[1] The vast biochemistry of nucleosides and nucleotides as coenzymes and secondary messengers offers unique opportunities for their emissive surrogates as biophysical and mechanistic tools. Pioneered by giants such as Leonard and Shugar, most early studies were done with perturbing emissive nucleoside analogues (e.g., 1,N^6-ethenoadenosine) or poorly emissive ones (e.g., 8-azapurines).[2,3] A key principle for the universal implementation of such probes is to minimize structural and functional perturbations, which are inevitable consequences of replacing any native residue with a synthetic analogue. We define nucleosides that fulfill such critical constraints as being isomorphic and isofunctional, respectively. To serve as effective emissive probes, at least one of the analogue's photophysical characteristics must respond to structural and environmental changes. We describe such an attribute as responsiveness.[4]

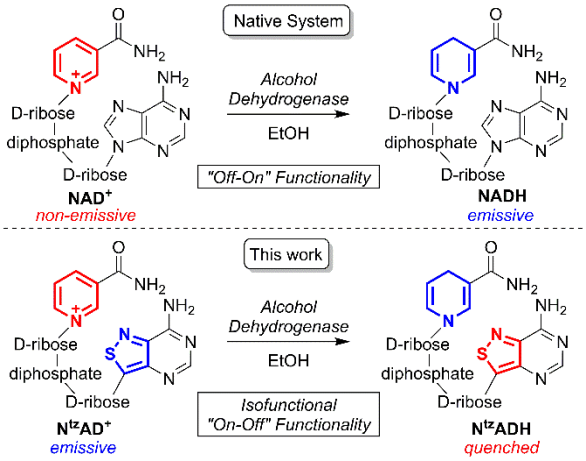

Figure 1. Comparing the photophysical behavior of native NAD^+ and $\mathbf{N^{tz}AD^+}$ in reactions involving alcohol dehydrogenase.

NAD^+ and NADH (Figure 1), the corresponding reduced form, are key determinants of the cellular redox state.[5] In addition to its metabolic roles and extracellular signaling functions,[6] NAD^+ is also a substrate for several key enzymes, including poly-ADP-ribose polymerases (PARP), mono-ADP-ribose transferases (ART), sirtuins, cyclases, and DNA ligases.[7,8,9,10] Its involvement in metabolic and regulatory processes make NAD^+ a key cofactor and its emissive analogues have been explored for decades.[11] One NAD^+ analogue that has been widely employed is 1,N^6-etheno NAD^+ (εNAD^+), originally introduced by Leonard and coworkers.[12] Enzymatic cleavage at the nicotinamide heterocycle (forming the corresponding nicotinamide and ε–adenosine diphosphate riboside) is required to induce a large change in εNAD^+'s emission quantum yield.[13,14,15] Other non-isomorphic fluorescent NAD^+ analogues have been developed for similar applications,[11b] and a clickable version was recently reported.[11c,16] Intriguingly, while the reduced native cofactor, NADH, is emissive (λ_{em} 460 nm, $\Phi = 0.02$),[17] the native NAD^+ is not. We thus sought to develop an isomorphic and isofunctional redox couple with orthogonal photophysical behavior to the native substrate (Figure 1). Such a synthetic cofactor could expand the processes that can be visualized in real-time by fluorescence spectroscopy.[18]

Our lab has developed a family of emissive isomorphic and isofunctional ribonucleosides based on an isothiazolo[3,4-*d*] pyrimidine core.[19] Considering the red-shifted absorption band and emissive nature of NADH relative to NAD^+,[17,20] we hypothesized that by replacing adenosine with $\mathbf{^{tz}A}$ (Figure 1, Scheme 1), our fluorescent adenosine analogue, an emissive NAD^+

analogue with distinct photophysical features and the potential to enhance the spectroscopic monitoring of NAD^+-dependent processes will be obtained.

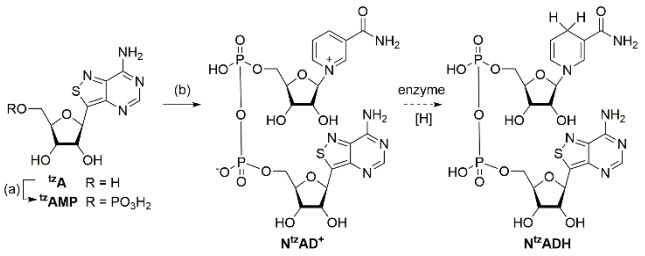

[a] *Reagents and conditions*: (a) $POCl_3$, Proton Sponge, trimethyl phosphate, 4 °C, 2 h, 50%. (b) i. β-Nicotinamide mononucleotide, CDI, Et_3N, DMF, rt, 6 h; ii. **^{tz}AMP**, DMF, rt, 4 days, 20%.[21]

Herein we report the synthesis, photophysics, and enzymatic interconversions of **$N^{tz}AD^+$**, an NAD^+ analogue based on our isomorphic isothiazolo heterocyclic system that is emissive and isofunctional. While the **$N^{tz}AD^+$/$N^{tz}ADH$** couple is complementary in its photophysical behavior to that of the native cofactors NAD^+/NADH, the emissive **$N^{tz}AD^+$** facilitates the fluorescence-based monitoring of ADP-ribosylation reactions, which are "fluorescently-silent" with the native cofactor.

To prepare **$N^{tz}AD^+$**, the previously synthesized **^{tz}A**[19] was treated with $POCl_3$ and trimethyl phosphate to give **^{tz}AMP** (Scheme 1), which was coupled to activated β-nicotinamide mononucleotide following published protocols.[11c,21] The spectroscopic properties of **$N^{tz}AD^+$** closely resemble that of **^{tz}A**, the core nucleoside. The absorption and emission maxima are found to be 336 and 411 nm, respectively, with a fluorescence quantum yield of 3.8 ± 0.4% (Table 1).

The biocompatibility and photophysical responsiveness of **$N^{tz}AD^+$**, was initially tested with *S. cerviseae* alcohol dehydrogenase (ADH). This dehydrogenase catalyzes the reversible oxidation of ethanol to acetaldehyde, using NAD^+ as a cofactor (Figure 2a).

Table 1. Photophysical properties

	λ_{abs} (ε)[a]	λ_{em} (Φ)[a]	Stokes shift[a]
^{tz}A[b]	338 (7.79)	410 (0.05)	5.23
$N^{tz}AD^+$[c]	336 (6.9)	411 (0.038)	5.41
$N^{tz}AD^+$[d]	338 (7.2)	411 (0.044)	5.23
$N^{tz}ADH$[d e]	336 (10.7)	412 (0.015)	5.49
NAD^+[b]	259 (16.9)	-	-
NADH[b]	339 (6.22)	460 (0.02)	7.76

[a] λ_{abs}, ε, λ_{em} and Stokes shift are in nm, 10^3 M^{-1} cm^{-1}, nm and 10^3 cm^{-1}, respectively. All values reflect the average of at least three independent measurements. See Table S1 for experimental errors. [b] See references 17 and 19. [c] Measured in MilliQ water [d] Measured in Tris buffer pH 7.6. [e] Measured at ADH reaction end, assuming complete consumption, Tris buffer pH 7.6.

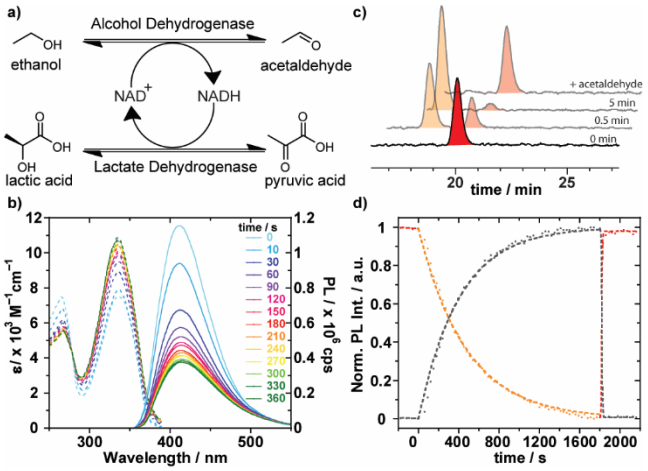

Figure 2. (a) Enzymatic cycle for NAD^+ consumption and regeneration with ADH and LDH. (b) ADH-mediated oxidation of ethanol to acetaldehyde using $\mathbf{N^{tz}AD^+}$ followed by UV and fluorescence spectroscopies (λ_{ex} = 330 nm). (c) As in b, showing $\mathbf{N^{tz}AD^+}$ (red) to $\mathbf{N^{tz}ADH}$ (orange) conversion, followed by HPLC (monitored at 330 nm). (d) ADH-mediated oxidation of ethanol to acetaldehyde followed by LDH-mediated reduction of pyruvic acid to lactic acid with $\mathbf{N^{tz}AD^+}$ (red/orange) and NAD^+ (grey) followed by real-time emission at 410 nm (λ_{ex} = 330 nm) and 465 nm (λ_{ex} = 335 nm), respectively. Dashed lines represent weighted curve fits.[21]

When subjecting $\mathbf{N^{tz}AD^+}$ to ADH and ethanol in buffer (pH 7.6), the conversion to the corresponding $\mathbf{N^{tz}ADH}$ was effectively monitored via a large decrease in its visible fluorescence intensity (λ_{ex} 330 nm, λ_{em} 410 nm) and increase in absorbance at 330 nm (Figure 2b).[21]

Subjecting NAD^+ to the same enzymatic reaction with ADH under the same conditions yielded a comparable rate with $t_{½}$ = 23±3 and 21±1 s for NAD^+ and $\mathbf{N^{tz}AD^+}$, respectively (Figure S4 and Table S2). The reaction was then reversed by adding excess acetaldehyde after the initial dehydrogenation was complete. The fluorescence signal was restored within seconds (Figure S5). Similarly, HPLC reaction monitoring showed near-full conversion of $\mathbf{N^{tz}AD^+}$ to $\mathbf{N^{tz}ADH}$ after 5 min followed by instantaneous regeneration of the former following the addition of acetaldehyde (Figure 2c).[21]

To further challenge our emissive NAD^+ analogue and assess its biochemical compatibility, it was tested with lactate dehydrogenase (LDH), a metabolic enzyme catalyzing the interconversion of pyruvate to lactate and concurrently NADH to NAD^+.[22] After consumption of $\mathbf{N^{tz}AD^+}$ with ADH and ethanol, the reaction is treated with pyruvic acid followed by LDH. The reformation of $\mathbf{N^{tz}AD^+}$ from $\mathbf{N^{tz}ADH}$ shows nearly full restoration of fluorescence intensity (Figure 2d, red/orange). This behavior was complementary to that of NAD^+, essentially mirroring its time course, which shows enhanced emission at 465 nm, arising from the formation of NADH, followed by a subsequent decrease in emission after the addition of LDH (Figure 2d, grey).

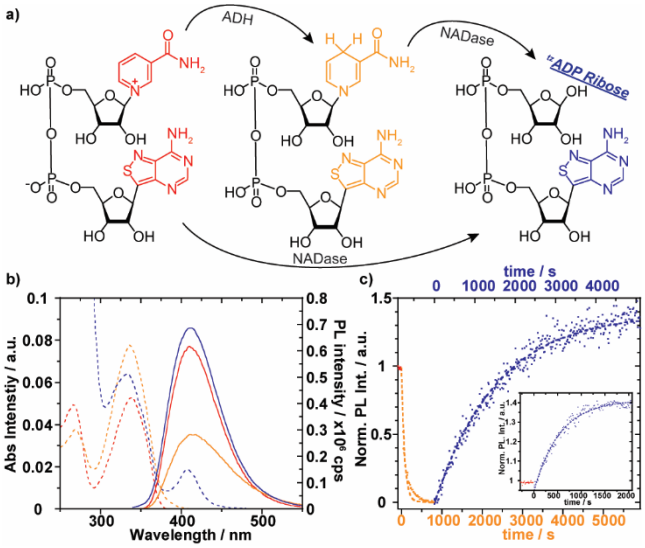

Figure 3. (a) Enzymatic cycle for $\mathbf{N^{tz}AD^+}$ consumption by ADH and NADase. (b) UV-Vis and emission (λ_{ex} = 330 nm) spectra of $\mathbf{N^{tz}AD^+}$ at time 0 (red), after oxidizing ethanol to acetaldehyde with ADH (orange) and subsequent treatment with NADase (blue). (c) Real-time emission intensity at 410 nm (λ_{ex} = 330 nm) of the enzymatic oxidation of ethanol to acetaldehyde by ADH with $\mathbf{N^{tz}AD^+}$ (orange, bottom time scale) followed by cleavage with NADase (blue, top time scale). Inset: Cleavage of $\mathbf{N^{tz}AD^+}$ with NADase (blue) followed by real-time emission at 410 nm (λ_{ex} = 330 nm).

To shed light on the photophysical behavior of $\mathbf{N^{tz}AD^+}$ and $\mathbf{N^{tz}ADH}$, their response upon enzymatic cleavage of the nicotinamide moiety with *porcine brain* NADase was evaluated (Figure 3). NADase specifically cleaves NAD^+ at the nicotinamide-ribose linkage, yielding nicotinamide and ADP-ribose (ADPR).[12,23] Treating $\mathbf{N^{tz}ADH}$ (generated from $\mathbf{N^{tz}AD^+}$ with ADH and ethanol) with NADase yielded a net 30% emission enhancement above the initial level before treatment with ADH (Figure 3b and 3c). Upon treatment of $\mathbf{N^{tz}AD^+}$ with NADase, a 40% increase in emission was observed (Figure 3c, inset). We hypothesize that the diminished emission observed upon reducing $\mathbf{N^{tz}AD^+}$ to $\mathbf{N^{tz}ADH}$ could arise from static quenching or a filtering effect by the reduced nicotinamide moiety, which in NADH absorbs at nearly the same wavelength as $\mathbf{^{tz}A}$ (Table 1). The observed emission enhancement upon treatment with NADase and subsequent conversion to $\mathbf{^{tz}ADP\ Ribose}$ (Figure 3) suggests, however, that the photophysics of these molecules is influenced by a myriad of intramolecular ground and excited state interactions between the nicotinamide and $\mathbf{^{tz}A}$ moieties. These may include a combination of filter effects, photoinduced electron transfer (PET), and additional quenching pathways arising from proximity-driven interactions between the nicotinamide and isothiazolo-pyrimidine core, as reported for NAD^+ and related analogues.[13a,17,20,24]

Finally, to illustrate the unique features of the emissive $\mathbf{N^{tz}AD^+}$ compared to the non-emissive NAD^+ and take advantage of the photophysical changes induced upon cleavage of the nicotinamide moiety, we have expanded the enzymatic processes monitored

to ADP ribosyl transfer reactions.[25] While several enzyme classes exploit NAD^+ through cleavage of the nicotinamide (e.g., PARPs, sirtuins), we employed arginine-specific mono-ADP-ribose transferases (ARTs), as they facilitate clearer detection of reactivity and biocompatibility. Two commercially available proteins with reported mono-ADP-ribosylation activity were used: human ART5, a transferase originally cloned from Yac-1 lymphoma cells in mice,[26] and Cholera toxin subunit A (CTA),[27] derived from Cholera toxin, a protein from the AB_5 toxin family. While arginine-specific ARTs operate in diverse biological systems and are regulated in complex manners,[25, 28] we chose ART5 as it has been identified as a major producer of arginine-specific ADP-ribose modification[29] and CTA, as it has been well-studied as an arginine-specific ADPR transferase.[30]

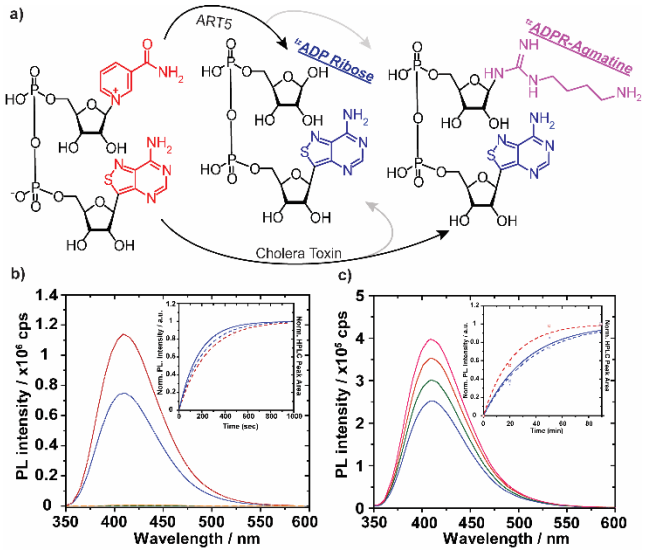

Figure 4. (a) Treatment of $\mathbf{N^{tz}AD^+}$ with ART5 and CTA to yield ADPR and ADPR-agmatine, respectively. (b) Steady state emission spectra following treatment of $\mathbf{N^{tz}AD^+}$ with ART5[21] at 0 (blue) and 18 min (red), as well as NAD^+ at 0 (green) and 18 min (orange), λ_{ex} = 335 nm; Inset: Fluorescence based kinetics of aforementioned reaction (λ_{em} = 410 nm, λ_{ex} = 335 nm, blue solid), and normalized HPLC-monitored product formation from reactions with $\mathbf{N^{tz}AD^+}$ (blue, dashed) and native NAD (red, dashed). (c) Steady state emission spectra (λ_{ex} = 335 nm) following treatment of $\mathbf{N^{tz}AD^+}$ with CTA;[21] reaction sampled at 0 (blue), 20 (green), 50 (orange), and 90 min (pink); Inset: Reactions with CTA following normalized emission intensity at 410 nm (λ_{ex} = 335 nm, blue, solid), normalized HPLC-monitored product formation from reactions with $\mathbf{N^{tz}AD^+}$ (blue, dashed) and native NAD^+ (red, dashed).[21]

Upon treatment with ART5 and agmatine (a commonly used Arg surrogate in ART assays),[29] both NAD^+ and $\mathbf{N^{tz}AD^+}$ were found to primarily undergo hydrolysis, under a variety of conditions, forming ADP Ribose and **^{tz}ADP Ribose**, respectively (Figure 4). This process, which has been documented for NAD^+,[26a,29] was found to occur at the same rate (Figure 4b), as detected via emission (for $N^{tz}AD^+$) and HPLC (for both NAD^+ and $N^{tz}AD^+$).[31] Upon treatment with CTA and agmatine, both NAD^+ and $\mathbf{N^{tz}AD^+}$ were found to produce primarily **ADPR-agmatine** and **^{tz}ADPR-agmatine**, respectively, as monitored via emission (for $\mathbf{N^{tz}AD^+}$) and HPLC (for both NAD^+ and $\mathbf{N^{tz}AD^+}$) (Figure 4c). These reactions show complete consumption of the corresponding substrates within 90 minutes, and formation of roughly 10% of hydrolyzed ADPR or **^{tz}ADPR** as a minor product. $\mathbf{N^{tz}AD^+}$ seemed to react slightly slower than the native cofactor with CTA. Importantly, however, **^{tz}ADPR-agmatine** was found to have near identical photophysical properties as **^{tz}A**, thus facilitating the fluorescence-based monitoring of the enzyme-mediated ADP-ribosylation.[32]

While the reactions of $\mathbf{N^{tz}AD^+}$ with alcohol and lactate dehydrogenase exemplify the isofunctionality of our emissive cofactor within the context of biochemically-relevant redox reactions, its reactivity with mono ADP-ribose transferases reinforces this notion. In particular, the suitability of $\mathbf{N^{tz}AD^+}$ as a substrate for ADP ribosyl transferases, key enzymes responsible for diverse post-transcriptional modifications of cellular regulatory significance,[25] illustrated with CTA-mediated **^{tz}ADP**-ribosylation of agmatine, showcases the formation of a new glycoside linkage to an amino acid derivative. Above all and in stark contrast to the non-emissive native NAD^+, such processes yield fluorescent ribosylated products and can be kinetically monitored by enhanced fluorescence signals, due to the displacement of the quenching nicotinamide moiety.

In summary, the isothiazolo[4,3-*d*]pyrimidine-based NAD^+ analogue displays isofunctionality and complementary photophysical behavior when compared to its native counterpart, with the oxidized form ($\mathbf{N^{tz}AD^+}$) being much more emissive than the reduced one (**N^{tz}ADH**). To our knowledge, no fluorescent NAD^+ analogues with photophysical behavior complementary to the native NAD^+ and NADH couple have been previously reported. Furthermore, $\mathbf{N^{tz}AD^+}$ serves as faithful substrate for ADP-ribose transferases. Unlike the non-emissive NAD^+, $\mathbf{N^{tz}AD^+}$ facilitates the kinetic monitoring of the enzymatic hydrolysis and transferase activity by fluorescence spectroscopy and yields visibly fluorescent products. $\mathbf{N^{tz}AD^+}$ has thus been subjected to five enzymes, which share common mechanistic pathways with most other NAD^+-utilizing reactions, where the nicotinamide moiety serves as

either a redox unit or as a leaving group. A synthetic cofactor such as **N^{tz}AD^{+}**, with unprecedented photophysical responses and biocompatibility, could therefore enhance and expand the real-time visualization of cofactor-dependent processes by fluorescence spectroscopy.

ASSOCIATED CONTENT

Supporting Information

Synthetic and analytical details, photophysical data, enzymatic protocols and HPLC traces. This material is available free of charge via the Internet at http://pubs.acs.org.

AUTHOR INFORMATION

Corresponding Author

ytor@ucsd.edu

Notes

Yitzhak Tor provides consulting services to TriLink Biotechnologies. The terms of the arrangements have been reviewed and approved by UCSD in accordance with its conflict of interest policies.

ACKNOWLEDGMENT

We thank the National Institutes of Health for generous support (GM 069773) and UCSD's Chemistry and Biochemistry MS Facility.

REFERENCES

1. Sinkeldam, R. W.; Greco, N. J.; Tor, Y., *Chem. Rev.* **2010,** *110*, 2579-2619.
2. Leonard, N. J. B., J. R., *Crit. Rev. Biochem.* **1984,** *15*, 125-199.
3. Wierzchowski, J.; Antosiewicz, J. M.; Shugar, D., *Mol. BioSyst.* **2014,** *10*, 2756-2774.
4. Sinkeldam, R. W.; Tor, Y., *Org. Biomol. Chem.* **2007,** *5*, 2523-2528.
5. (a) Everse, J.; Anderson, B.; You, K., *The Pyridine nucleotide coenzymes*. Academic Press: New York, 1982; (b) Ying, W. H., *Antioxid. Redox Signaling* **2008,** *10*, 179-206; (c) Collins, Y.; Chouchani, E. T.; James, A. M.; Menger, K. E.; Cocheme, H. M.; Murphy, M. P., *J. Cell Sci.* **2012,** *125*, 801-806.
6. Garten, A.; Schuster, S.; Penke, M.; Gorski, T.; de Giorgis, T.; Kiess, W., *Nat. Rev. Endocrinol.* **2015,** *11*, 535-546.
7. (a) Chambon, P.; Mandel, P.; Weill, J. D., *Biochem. Biophys. Res. Commun.* **1963,** *11*, 39-43; (b) Hayaishi, O.; Ueda, K., *Annu. Rev. Biochem* **1977,** *46*, 95-116; (c) Cervantes-Laurean, D.; Minter, D. E.; Jacobson, E. L.; Jacobson, M. K., *Biochemistry* **1993,** *32*, 1528-1534; (d) Hassa, P. O.; Haenni, S. S.; Elser, M.; Hottiger, M. O., *Microbiol. Mol. Biol. Rev.* **2006,** *70*, 789-829.
8. (a) Boulikas, T., *Anticancer Res.* **1991,** *11*, 489-527; (b) Hottiger, M. O., *Annu. Rev. Biochem.* **2015,** *84*, 227-263.
9. Bonkowski, M. S.; Sinclair, D. A., *Nat. Rev. Mol. Cell Biol.* **2016,** *17*, 679-690.
10. Moss, J.; Stanley, S. J., *J. Biol. Chem.* **1981,** *256*, 7830-3.
11. (a) Pankiewicz, K. W.; Watanabe, K. A.; Lesiak-Watanabe, K.; Goldstein, B. M.; Jayaram, H. N., *Curr. Med. Chem.* **2002,** *9*, 733-741; (b) Pergolizzi, G.; Butt, J. N.; Bowater, R. P.; Wagner, G. K., *Chem. Commun.* **2011,** *47*, 12655-12657; (c) Wang, Y.; Rosner, D.; Grzywa, M.; Marx, A., *Angew. Chem., Int. Ed.* **2014,** *53*, 8159-8162.
12. Barrio, J. R.; Secrist, J. A.; Leonard, N. J., *Proc. Natl. Acad. Sci. U. S. A.* **1972,** *69*, 2039-2042.
13. (a) Gruber, B. A.; Leonard, N. J., *Proc. Natl. Acad. Sci. U. S. A.* **1975,** *72*, 3966-3969; (b) Luisi, P. L.; Baici, A.; Bonner, F. J.; Aboderin, A. A., *Biochemistry* **1975,** *14*, 362-368.
14. Lee, C.-Y.; Everse, J., *Arch. Biochem. Biophys.* **1973,** *157*, 83-90.
15. To our knowledge, the enzymatic conversion of εNAD^{+} to εNADH has not been photophysically studied. The cofactors have shown photophysical differences when bound to GDH: Dieter, H.; Koberstein, R.; Sund, H., *FEBS. Lett.* **1974**, *47*, 90-93.
16. Willner has electrochemically studied surface-bound cofactors; See: (a) Bardea, A.; Katz, E.; Bückmann, A. F.; Willner, I., *J. Am. Chem. Soc.* **1997**, *119*, 9114-9119; (b) Katz, E.; Willner, I., *Angew. Chem. Int. Ed.* **2004**, *43*, 6042-6108.
17. Scott, T. G.; Spencer, R. D.; Leonard, N. J.; Weber, G., *J. Am. Chem. Soc.* **1970,** *92*, 687-695.
18. (a) Vranken, C.; Fin, A.; Tufar, P.; Hofkens, J.; Burkart, M. D.; Tor, Y., *Org. Biomol. Chem.* **2016**, *14*, 6189-6192; (b) Deen, J.; Vranken, C.; Leen, V.; Neely, R. K.; Janssen, K. P. F.; Hofkens, J., *Angew. Chem. Int. Ed.* **2017**, *56*, 5182-5200.
19. (a) Rovira, A. R.; Fin, A.; Tor, Y., *J. Am. Chem. Soc.* **2015,** *137*, 14602-14605; (b) Rovira, A. R.; Fin, A.; Tor, Y., *Chem. Sci.* **2017,** *8*, 2983-2993.
20. Hull, R. V.; Conger III, P. S.; Hoobler, R. J., *Biophys. Chem.* **2001,** *90*, 9-16.
21. See supporting information for experimental details.
22. (a) Månsson, M.-O.; Larsson, P.-O.; Mosbach, K., *FEBS Lett.* **1979,** *98*, 309-313; (b) Chenault, H. K.; Whitesides, G. M., *Bioorg. Chem.* **1989,** *17*, 400-409; (c) Faber, K., *Biotransformations in organic chemistry*. Springer-Verlag: Berlin ; New York, 1992.
23. Kaplan, N. O.; Colowick, S. P.; Nason, A., *J. Biol. Chem.* **1951,** *191*, 473-483.
24. Tanaka, M.; Ohkubo, K.; Fukuzumi, S., *J. Phys. Chem. A* **2006,** *110*, 11214-11218.
25. *Endogenous ADP-Ribosylation*; Koch-Nolte, F., Ed.; Springer International Publishing: 2015.
26. (a) Weng, B. Y.; Thompson, W. C.; Kim, H. J.; Levine, R. L.; Moss, J., *J. Biol. Chem.* **1999,** *274*, 31797-31803; (b) Okazaki, I. J.; Moss, J., *Annu Rev Nutr* **1999,** *19*, 485-509.
27. Vanden Broeck, D.; Horvath, C.; De Wolf, M. J., *Int. J. Biochem. Cell Biol.* **2007,** *39*, 1771-5.
28. (a) Moss, J.; Stanley, S. J.; Osborne, J. C., Jr., *J. Biol. Chem.* **1981,** *256*, 11452-6; (b) Hottiger, M. O.; Hassa, P. O.; Luscher, B.; Schuler, H.; Koch-Nolte, F., *Trends Biochem. Sci* **2010,** *35*, 208-219.
29. Glowacki, G.; Braren, R.; Firner, K.; Nissen, M.; Kuhl, M.; Reche, P.; Bazan, F.; Cetkovic-Cvrlje, M.; Leiter, E.; Haag, F.; Koch-Nolte, F., *Protein Sci.* **2002,** *11*, 1657-1670.
30. (a) Moss, J.; Vaughan, M., *J. Biol. Chem.* **1977,** *252*, 2455-2457; (b) Tsai, S. C.; Noda, M.; Adamik, R.; Moss, J.; Vaughan, M., *Proc. Natl. Acad. Sci. U.S.A.* **1987,** *84*, 5139-42.
31. High levels of glycohydrolase activity versus transferase activity have been reported for ART5. See reference 29.
32. **^{tz}ADP-ribose** and **^{tz}ADPR-agmatine** have the same photophysical properties as **^{tz}A**, the parent nucleoside. See SI and Figures S9 and S15.